

*Complementary Supporting Information's*

**Solution-processed bulk heterojunction solar cells with silyl end-capped sexithiophene**

Jung Hei Choi, Mohamed E. El-Khouly, Taehee Kim, Youn Su Kim, Dae Won Cho, Ung Chan Yoon, Shunichi Fukuzumi, and Kyungkon Kim

**Caption Figures**

Fig. S1. Steady-state fluorescence spectra of **DH-6T** and **DSi-6T** in benzonitrile;  $\lambda_{\text{ex}} = 415 \text{ nm}$ .

Fig. S2. DPV voltammograms of **DSi-6T**, **DH-6T** and PCBM in deaerated benzonitrile. Scan rate =  $50 \text{ mV s}^{-1}$ .

Fig. S3. CV of **DH-6T** in deaerated benzonitrile. Scan rate =  $50 \text{ mV s}^{-1}$ .

Fig. S4. CV of **DSi-6T** in deaerated benzonitrile. Scan rate =  $50 \text{ mV s}^{-1}$ .

Fig. S5. CV of **PCBM** in deaerated benzonitrile. Scan rate =  $50 \text{ mV s}^{-1}$ .

Fig. S6. (upper) Nanosecond transient spectra of **DSi-6T** (0.05 mM) in deaerated benzonitrile;  $\lambda_{\text{ex}} = 440 \text{ nm}$ . (lower) Decay-time profile of  ${}^3\text{DSi-6T}^*$  at 710 nm.

Fig. S7. Nanosecond transient spectra of **DH-6T** (0.05 mM) in the presence of PCBM (0.1 mM) in deaerated benzonitrile;  $\lambda_{\text{ex}} = 440 \text{ nm}$ . Inset: Decay-time profile of  ${}^3\text{DH-6T}^*$  (700 nm), and rise-profile of **DH-6T<sup>+</sup>** (800 nm).

Fig. S8. Nanosecond transient spectra of **DH-6T** (0.05 mM) in the presence of PCBM (0.05 mM) in deaerated benzonitrile;  $\lambda_{\text{ex}} = 440 \text{ nm}$ . Inset: Decay-time profile of  ${}^3\text{DH-6T}^*$  (700 nm), and rise-profiles of **DH-6T<sup>+</sup>** (800 and 1500 nm) and **PCBM<sup>-</sup>** (1000 nm).

Fig. S9. Dependence of rate constant of the formation of **DH-6T<sup>+</sup>** at 800 nm on concentration of PCBM in deaerated benzonitrile. Inset: First-order plot.

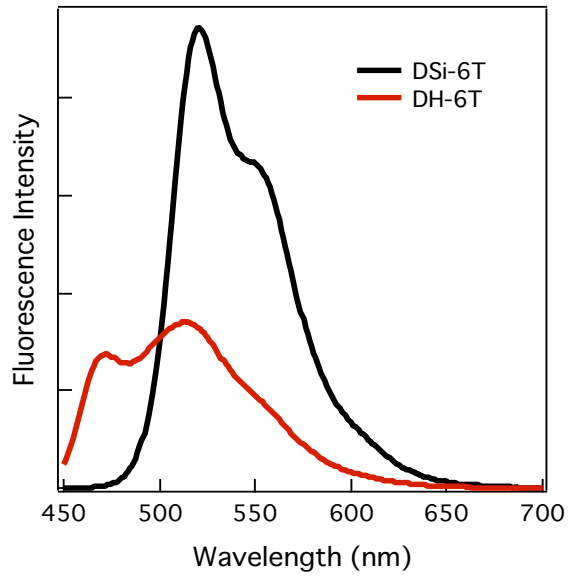


Fig. S1. Steady-state fluorescence spectra of **DH-6T** and **DSi-6T** in benzonitrile;  $\lambda_{\text{ex}} = 415$  nm.

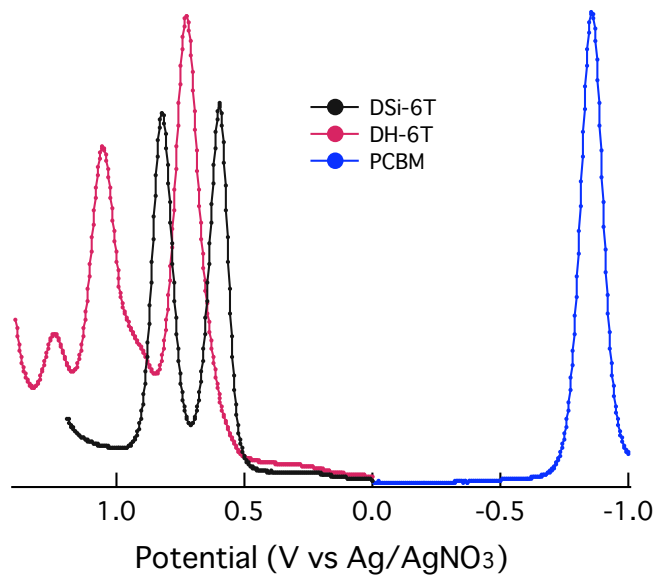


Fig. S2. DPV voltammograms of **DSi-6T**, **DH-6T** and **PCBM** in deaerated benzonitrile. Scan rate = 50 mV s<sup>-1</sup>.

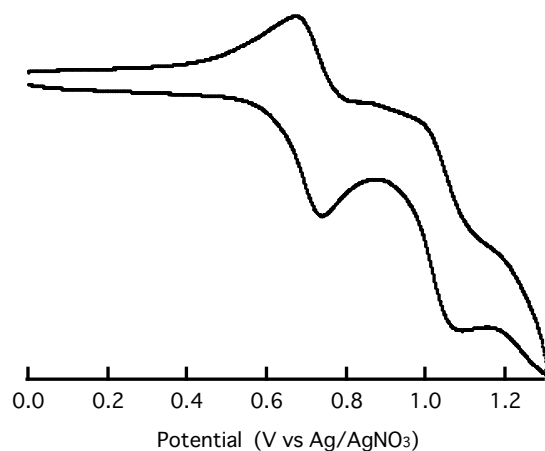


Fig. S3. CV of **DH-6T** in deaerated benzonitrile. Scan rate = 50 mV s<sup>-1</sup>.

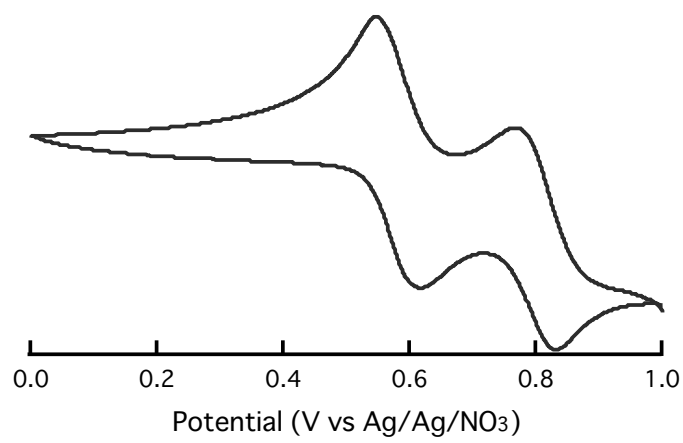


Fig. S4. CV of **DSi-6T** in deaerated benzonitrile. Scan rate = 50 mV s<sup>-1</sup>.

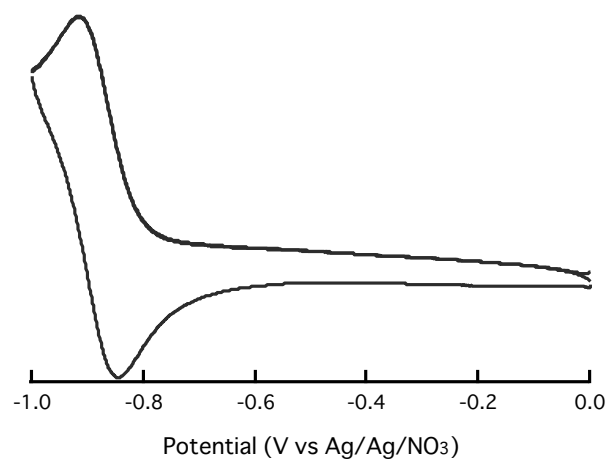


Fig. S5. CV of **PCBM** in deaerated benzonitrile. Scan rate = 50 mV s<sup>-1</sup>.

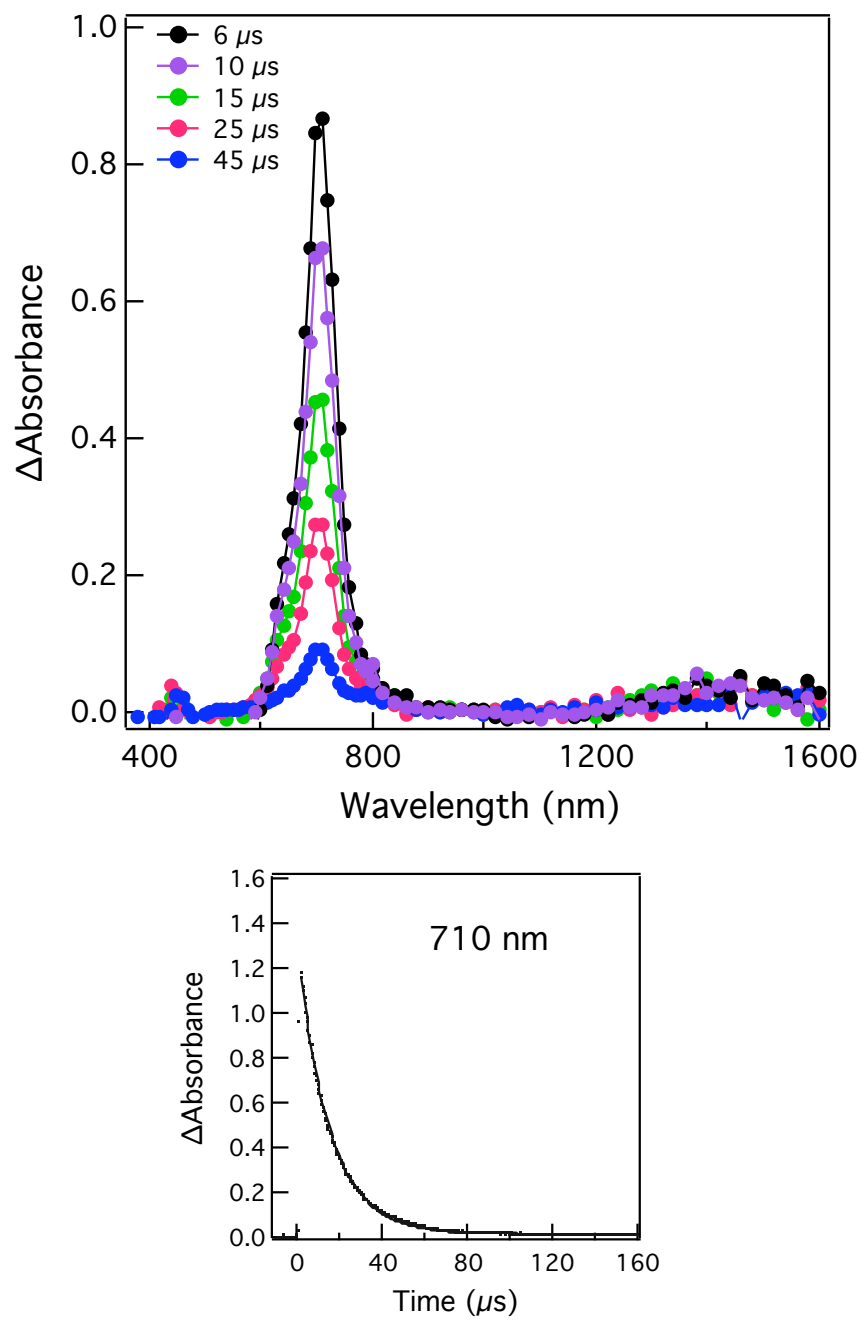


Fig. S6. (upper) Nanosecond transient spectra of **DSi-6T** (0.05 mM) in deaerated benzonitrile;  $\lambda_{\text{ex}} = 440$  nm. (lower) Decay-time profile of  ${}^3\text{DSi-6T}^*$  at 710 nm.

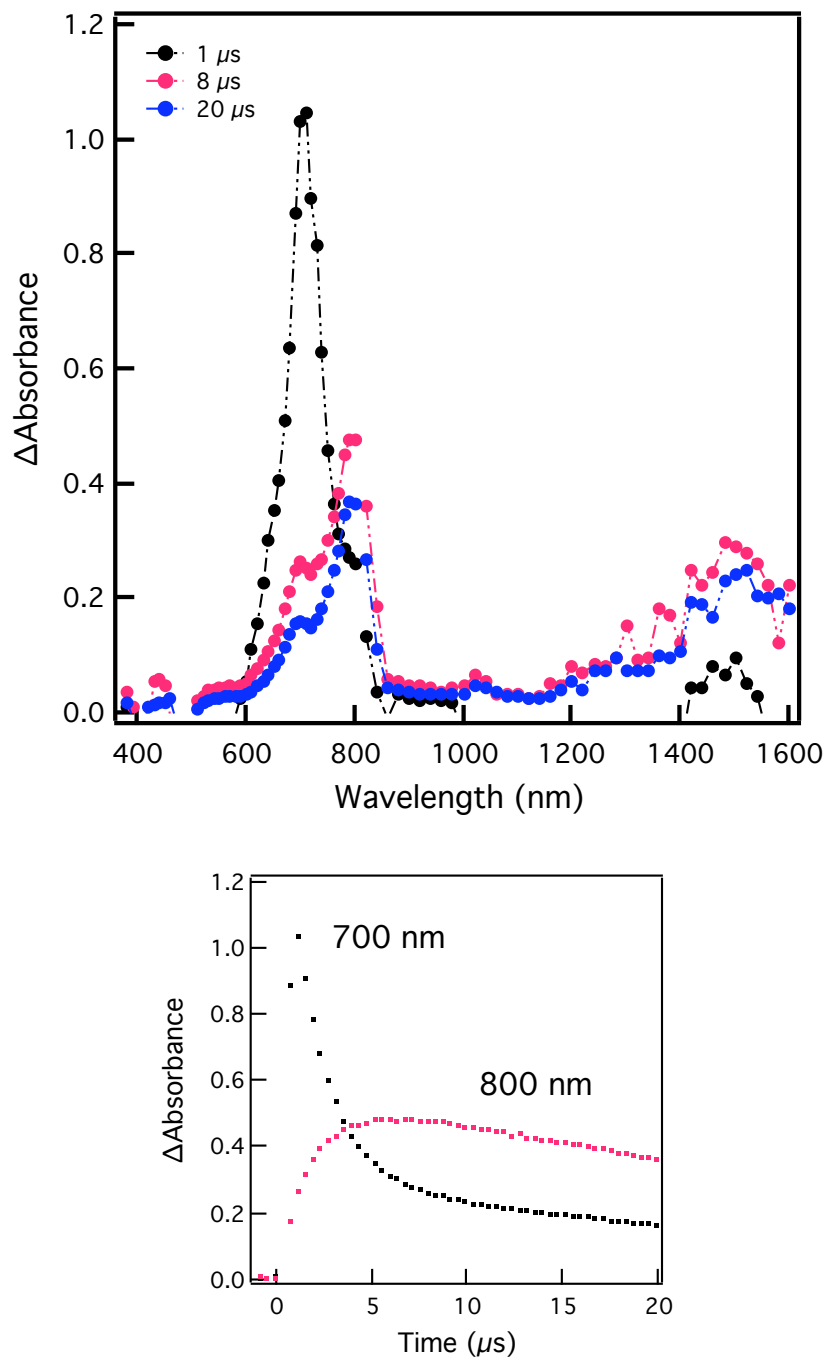


Fig. S7. Nanosecond transient spectra of **DH-6T** (0.05 mM) in the presence of PCBM (0.1 mM) in deaerated benzonitrile;  $\lambda_{\text{ex}} = 440$  nm. Inset: Decay-time profile of  ${}^3\text{DH-6T}^*$  (700 nm), and rise-profile of  $\text{DH-6T}^+$  (800 nm).

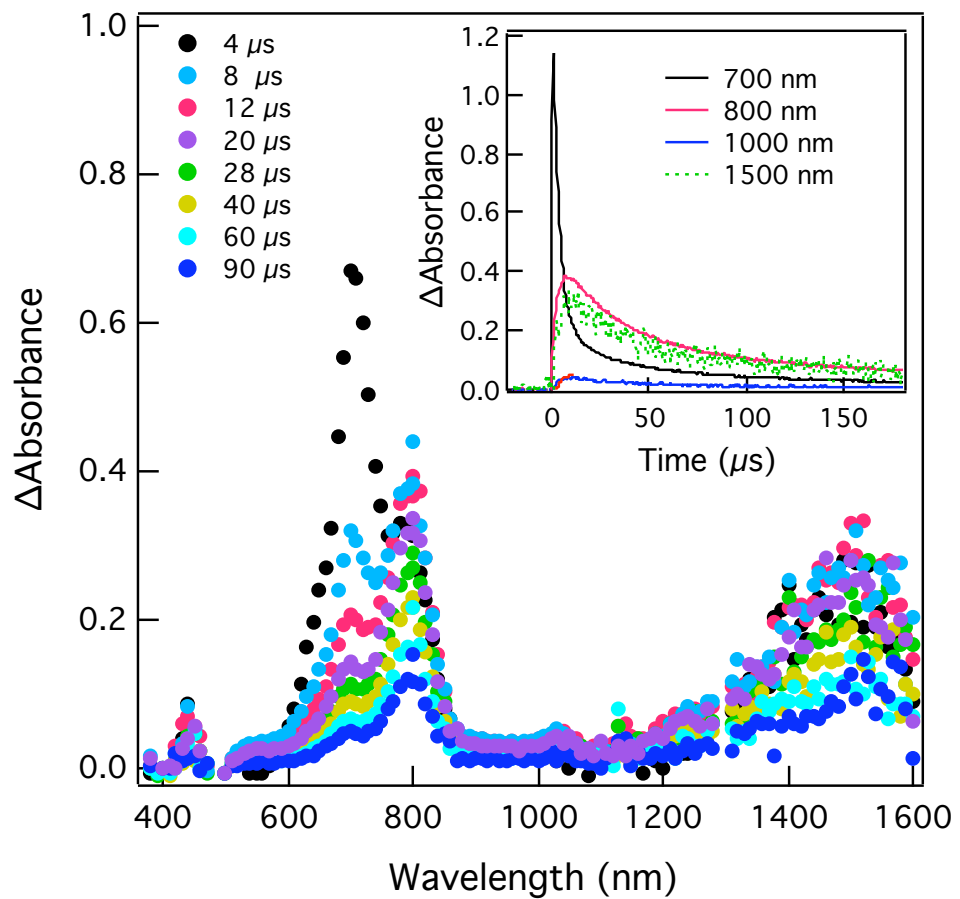


Fig. S8. Nanosecond transient spectra of **DH-6T** (0.05 mM) in the presence of **PCBM** (0.05 mM) in deaerated benzonitrile;  $\lambda_{\text{ex}} = 440$  nm. Inset: Decay-time profile of  ${}^3\text{DH-6T}^*$  (700 nm), and rise-profiles of  $\text{DH-6T}^{*+}$  (800 and 1500 nm) and  $\text{PCBM}^{-}$  (1000 nm).

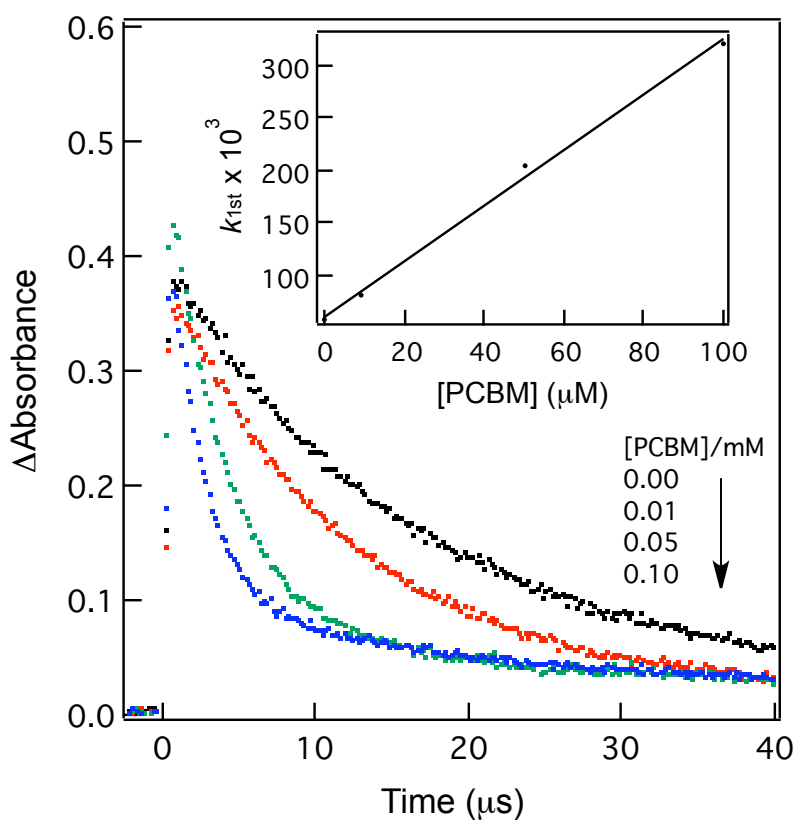


Fig. S9. Dependence of rate constant of the formation of **DH-6T<sup>+</sup>** at 800 nm on concentration of PCBM in deaerated benzonitrile. Inset: First-order plot.